Supporting Information

Thermo-processable covalent scaffolds with reticular hierarchical porosity and their high efficiency capture of carbon dioxide

Su-Young Moon,[a‡] Eunkyung Jeon,[a‡] Jae-Sung Bae,[a] Mi-Kyoung Park,[b] Chan Kim, [c] Do Young Noh, [a c] Eunji Lee[b] and Ji-Woong Park[*a]

[a] School of Materials Science and Engineering, Gwangju Institute of Science and Technology, 123 Cheomdan-gwagiro, Buk-gu, Gwangju, 500-712, Korea

[b] Graduate School of Analytical Science and Technology, Chungnam National University, Daejon, 305-764, Korea

[c] Department of Physics and Photon Science, Gwangju Institute of Science and Technology, 123 Cheomdan-gwagiro, Buk-gu, Gwangju, 500-712, Korea

E-mail: jiwoong@gist.ac.kr

TABLE OF CONTENTS

Experimental Section

Materials: All chemicals were purchased from Sigma-Aldrich. N,N,dimethylformamide (DMF) (anhydrous, 99.8%) was used without further purification. Hexamethylene diisocyanate (HDI) (98%) was distilled under reduced pressure. CO_2, N_2 and gas mixtures (CO_2/N_2=15/85, CO_2/N_2=0.2/99.8, and CO_2/CH_4=10/90 in %) were used as received (purity 99.999%) from Sinil Gas.

Characterization: Gas adsorption isotherms were recorded on an ASAP 2020 volumetric adsorption apparatus (Micromeritics) at 77 K and 298 K for nitrogen and 273 K and 298 K for carbon dioxide. Prior to analysis, the samples were degassed in the degas port of the adsorption analyzer at 473 K for at least 12 hours. The surface area, heat of adsorption, pore volume, and pore size distribution were analyzed using ASAP 2020 v3.00 software (Micromeritics).

Scanning electron microscopy (SEM) images were collected on a Hitachi S-4700. Before taking SEM measurements, samples were coated with ultrathin platinum by vacuum sputtering. Transmission electron microscopy (TEM) was carried out using a model JEM-2100 of JEOL. The samples used for TEM were embedded in epoxy resin and then sliced using a PowerTome-XL microtome to about 60-nm-thick sections. The sliced samples were placed onto a copper grid and stained with RuO_4 for 30 min.

^{1}H NMR spectra were recorded on a JEOL JNM-LA 400 WB FT-NMR in $CDCl_3$, and DMF-d_7 as solvents. Solid-state ^{13}C NMR data were acquired using an AVANCE 400 WB Bruker with a resonance frequency of 400 MHz and spin frequency of 7 KHz. Fourier transform infrared (FTIR) spectroscopy was carried out on a Perkin-Elmer 2000 Series instrument. Powder samples for FTIR were prepared using pellets in KBr.

Thermogravimetric analysis (TGA) of the samples was carried out using a TA Instruments 2100 series analyzer in the range of 20 ~ 800°C at a heating rate of 10 °C/min under nitrogen.

X-ray photoelectron spectroscopy (XPS) was performed at a 90° take-off angle with a Multilab 2000 (Thermo Electron Corporation) spectrometer using MgKα radiation (1253.6 eV) as the X-ray source, in an ultrahigh vacuum condition. The analyzed core level lines (C1s, O1s, N1s) were calibrated with respect to the C1s binding energy conventionally set here at 285 eV.

Adsorption-desorption cycles of CO_2 or a mixture of gases on RUNs were measured using a thermogravimetric analyzer (TA Instruments 2100 series). For the pure CO_2 and mixed gas (15 % or 0.2 % CO_2/N_2) recycling tests, the sample was activated under a N_2 stream at a flow rate of 20 mL/min at 100 °C for 30 min. After activation, the gas was then switched from N_2 to pure CO_2 (20 mL/min) or mixed gas (20 mL/min) and the change in weight of the sample with time was recorded at 25 °C. Once the sample was saturated with the adsorbed gas (i.e., CO_2 or mixed gas), the gas in the stream was switched back from pure CO_2 or mixed gas to N_2 (20 mL/min) and the temperature was increased to the target temperature at a heating rate of 10 °C/min. The sample was cooled to 25 °C under N_2 (20 mL/min), and the gas in the stream was again switched back to CO_2 or mixed gas for the next absorption run. This adsorption–desorption cycle was repeated several times.

Raman spectra were obtained from Renishaw InVia Raman Microscope with an excitation wavelength of 514 nm.

Elemental analysis were carried out using Thermofinnigan EA1112. Each sample was measured after dryig at 100 °C for 3hours.
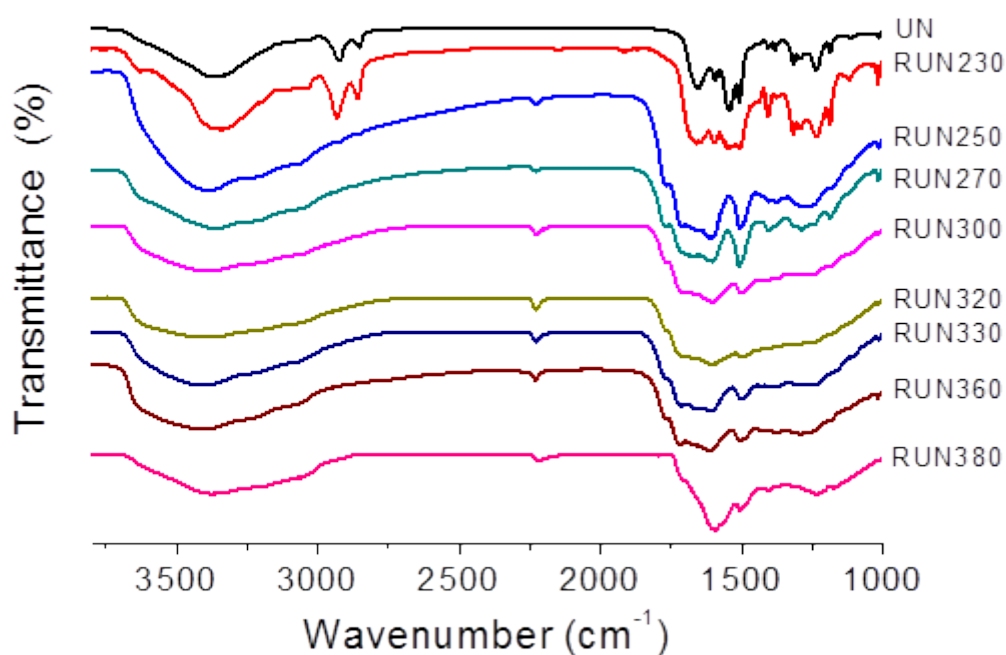
Fig. S1 FT-IR spectra of UN and RUNs treated at different T_r values: 230 °C, 250 °C, 270 °C, 300 °C, 320 °C, 330 °C, 360 °C, and 380 °C. All samples were pelletized in KBr for FT-IR. The absorption bands at 3335 cm^{-1}, 1655 cm^{-1}, 1542 cm^{-1}, and 1316 cm^{-1} were due to N-H stretching, C=O stretching, N-H bending, and C-N stretching vibrations of hydrogen-bonded urea, respectively.(2) The bands at 2930-2860 cm^{-1} and 3150-3050 cm^{-1} correspond to the aliphatic and aromatic C-H stretching vibrations, respectively. The bands at 1594 cm^{-1}, 1508 cm^{-1}, and 1406 cm^{-1} were due to C=C stretching vibrations in the aromatic ring. The peaks at 2260 cm^{-1}, 2155 cm^{-1} and 2230 cm^{-1} are attributed to the isocyanate N=C=O stretching, carbodiimide N=C=N stretching, and cyanamide C≡N stretching vibrations, respectively, which were generated during thermal dissociation and rearrangement of urea bonds.(3) The C=O stretching vibration of uretidinedione (isocyanate dimer) appeared at 1768 cm^{-1} and the absorption at 1711 cm^{-1} is attributed to the stretching vibration of isocyanurate C=O.(4)
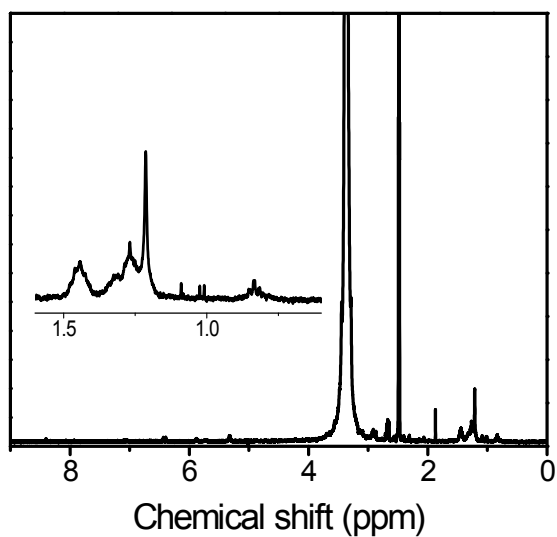
Fig. S2 ^{1}H NMR spectrum of condensates collected during thermal treatment of UN at 230 ℃ for 8 h under nitrogen flow.
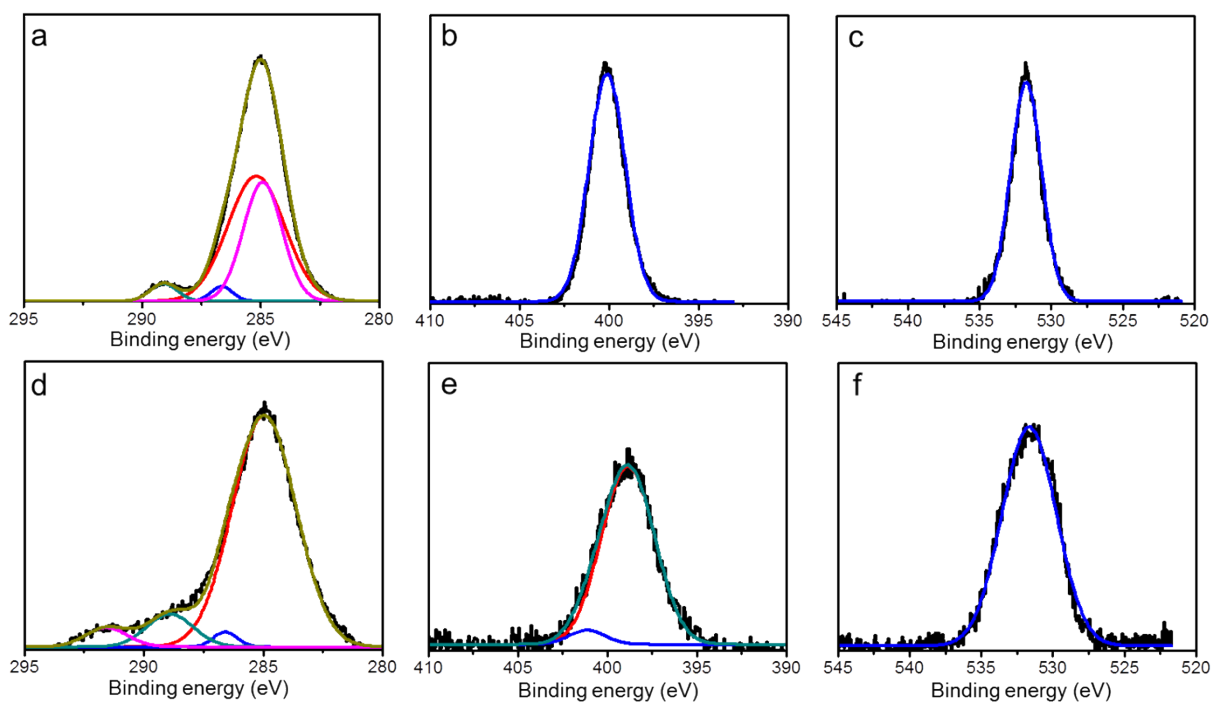

Fig. S3 XPS spectra of UN and RUN380. **a-c,** C1s, N1s, and O1s of UN, respectively. **d-f,** C1s, N1s, and O1s of RUN380, respectively. The peak assignments are given in **Table S1**.

Table S1. Assignment of the XPS data for UN and RUN380 in a to f in Figure S3.

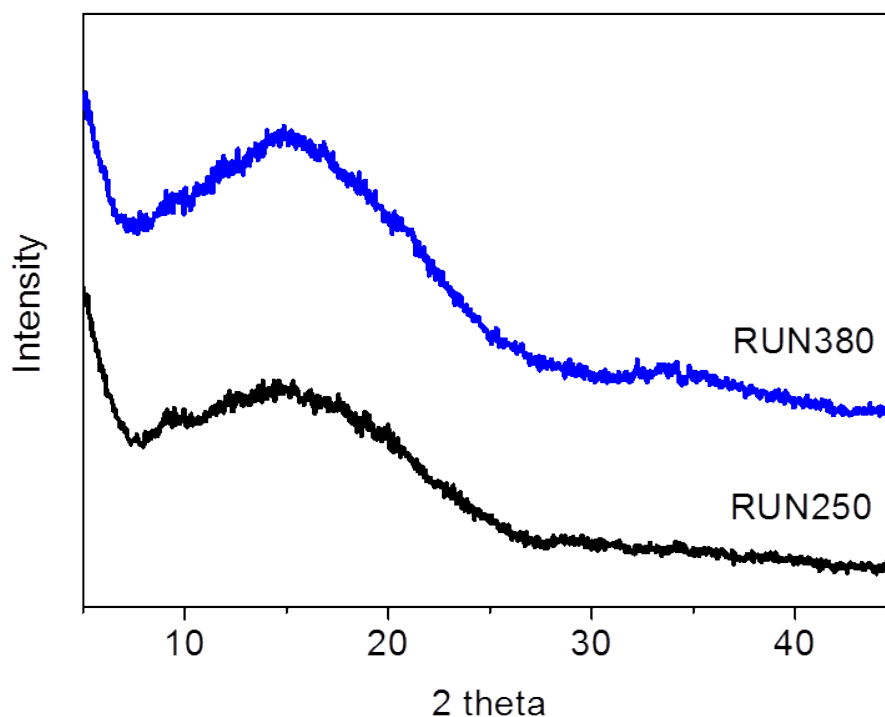|		Binding energy (eV) of UN			Binding Energy (eV) of RUN380
C1s	a	284.9 C=C/C-H	d		284.98 C-C/C-H
		285.2 C-C/C-H			282.23
		286.7 C-N			288.01 N-CN
		289.1 O=C-N			291.46 (π->π* shake-up)
N1s	b	400.1 NHC=O	e		398.9 Isocyanurate
					401.2 (RNH)$_2$C=O, (R=phenyl)
O1s	c	531.8 urea C=O	f		531.7 Urea/Isocyanurate C=O

Fig. S4 PXRD data indicating amorphous network structure for RUN250 and RUN380. The x-ray powder diffraction measurement was performed at the 5D GIST NCRC-CELA beamline of the Pohang Light Source-Ⅱ (PLS-Ⅱ) in Korea. The x-ray wavelength λ (x-ray energy) was fixed to 1.24 Å (10 keV) by a double-bounce Si (111) monochromator. The diffracted x-rays from specimen were measured by a scintillation point detector.
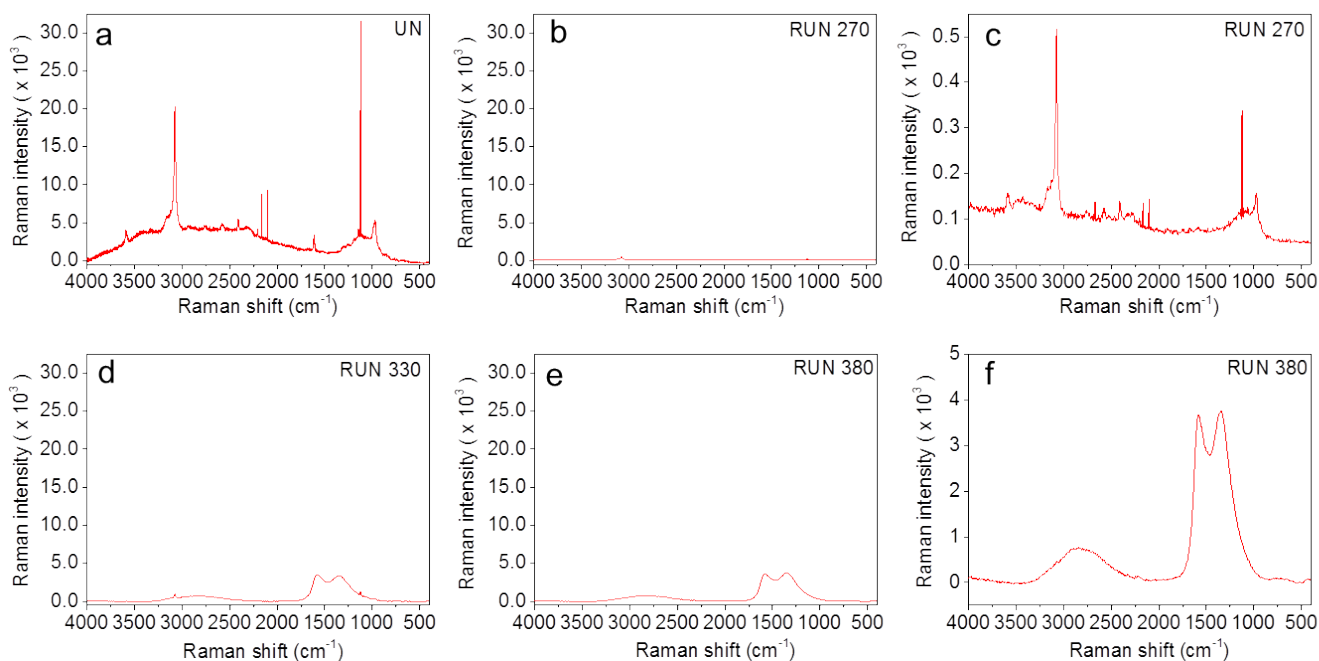
Fig. S5 Raman spectra of UN and RUN. Raman spectra for **a,** UN and **b-c,** RUN270 exhibits N-H stretching, aromatic C-H stretching , C=O stretching, N-C-N stretching vibrations and aromatic ring breathing motion at 3587 cm^{-1}, 3076 cm^{-1}, 1600 cm^{-1}, 967 cm^{-1} and 1122 cm^{-1}, respectively. **d,** RUN330 exhibits aromatic C-H stretching, N-C-N stretching vibrations and aromatic ring breathing motion at 3076 cm^{-1}, 967 cm^{-1} and 1122 cm^{-1}, respectively. The peaks at 1344 cm^{-1} and 1585 cm^{-1} correspond to D and G-band of partially carbonized UN, respectively. I_D/I_G ratio of RUN330 is 0.96. **d-f,** RUN380 exhibits a peak of cyanamide C≡N stretching vibrations at 2220 cm^{-1} as well as broad D and G peaks. The broad peak around 2834 cm^{-1} indicates the presence of significant structural defects of carbon. I_D/I_G ratio of RUN380 is 1.02. **c** and **f,** Magnified Raman spectra for RUN270 and RUN380, respectively.

Table S2. Elemental analysis data for UN and RUN.

Sample/Element	N (%)	C (%)	H (%)	O (%)	C/O	C/N	N/O
UN (Theo.)	15.6	68.7	6.8	8.9	7.7	4.4	1.7
RUN (Theo.)	11.6	71.9	3.3	13.2	5.5	6.2	0.90
UN	15.7	67.3	6.8	10.2	6.6	4.3	1.5
RUN270	12.5	66.9	3.4	17.2	3.9	5.4	0.73
RUN330	14.2	68.1	3.2	14.5	4.7	4.8	0.98
RUN380	14.5	65.8	3.0	16.1	4.1	4.5	0.90

Theoretical EA data for RUN was obtained by assuming that the RUN consist entirely of the isocyanurate network formed via cyclization of tetrakis(4-isocyanatophenyl)methane. EA data for RUN 270, 330, and 380 show that they became enriched with nitrogen and oxygen as compared with RUN(Theo).

Table S3. Summary of CO_2 adsorption at 273K in porous materials.

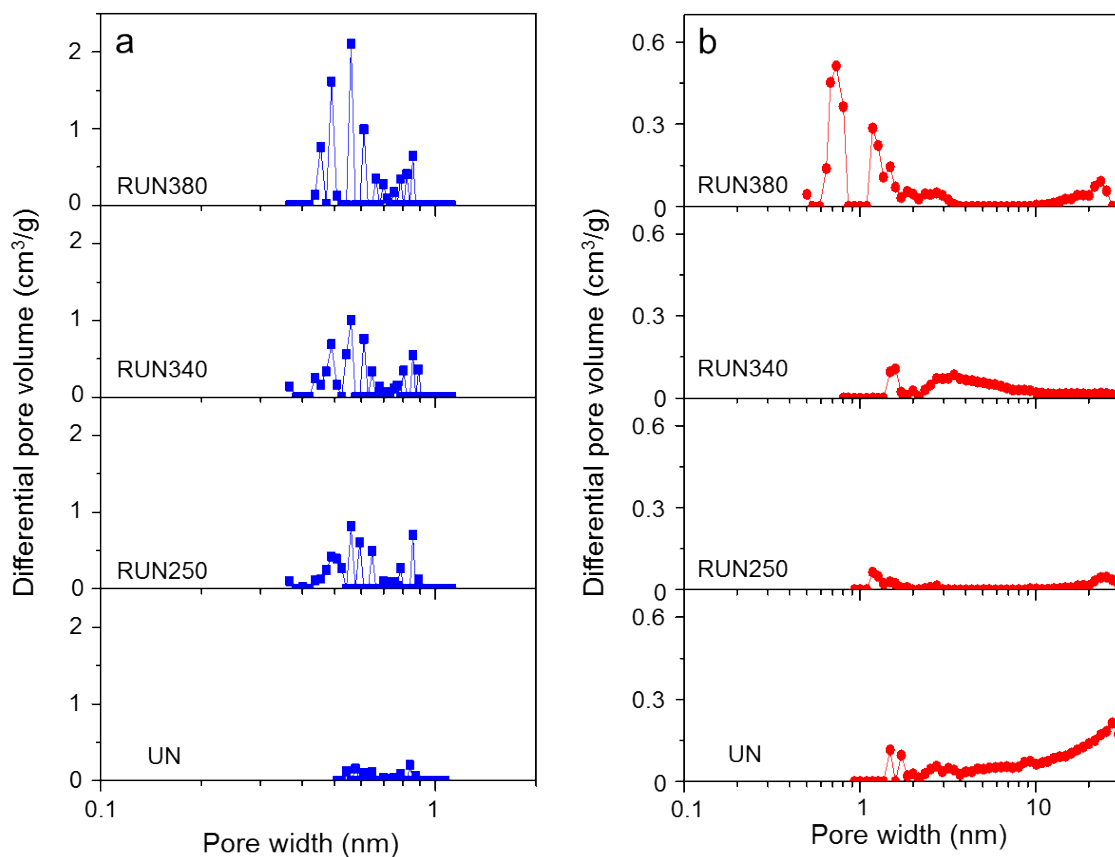| Frameworks	BET surface area (m²/g)	CO₂ adsorption (mmol/g)	Ref.
RUN380	408	3.6	This work
COF-1	750	2.32	6, 9
COF-5	1670	1.34	6, 9
COF-6	750	3.84	6, 9
COF-8	1350	1.43	6, 9
COF-10	1760	1.21	6, 9
COF-102	3620	1.56	6, 9
COF-103	3530	1.70	6, 9
POF-C-1000	785	3.54	7
POF-C-800	335	3.24	7
POF-DC-1000	100	2.07	7
POF (PAF-6)	177	1.81	7
PAF-1	5600	2.05	8, 9
PAF-3	2932	3.48	8, 9
PAF-4	2246	2.41	8, 9

Fig. S6 Pore-size distribution derived from adsorption data of **a,** CO_2 and **b,** N_2 for the UN and RUNs.
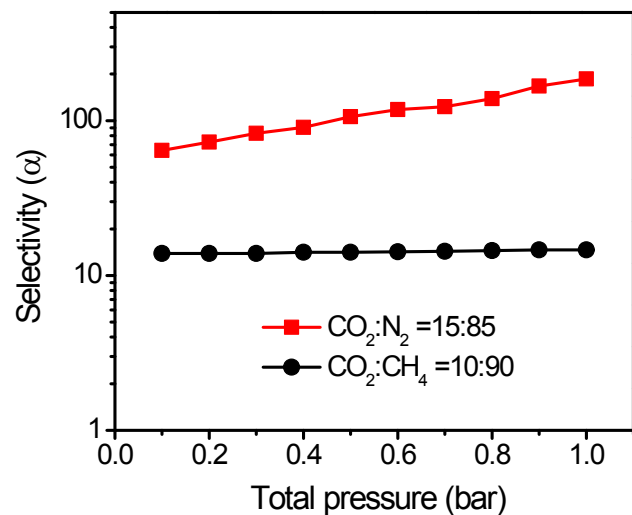
Fig. S7 The adsorption selectivity curves estimated according to the ideal adsorbed solution theory (IAST) for RUN380.(5) The single gas isotherms were fitted using the Langmuir model. The adsorption selectivities for binary mixtures were calculated using the Ideal Adsorption Solution Theory (IAST) of Myers and Prausnitz. The IAST calculations were carried out for binary mixture containing 15% CO_2 in N_2 and 10% CO_2 in CH_4 which are similar compositions with flue gas and natural gas, respectively. The adsorption selectivities of RUN380 for CO_2 relative to CH_4 and relative to N_2 were, respectively, $\alpha_{CO2/CH4}$=15 and $\alpha_{CO2/N2}$=186, at 298K and 1 bar.

Table S4. Summary of adsorption selectivities for 15/85 CO_2/N_2 mixture at 1bar and 296K using the ideal adsorbed solution theory (IAST). (10)

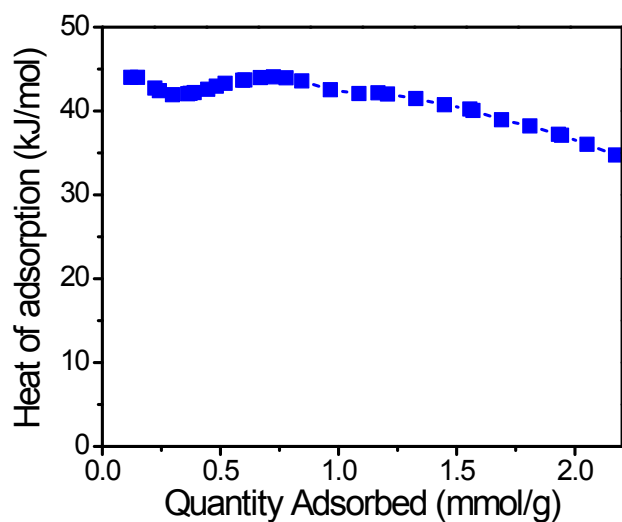| Frameworks	CO_2 uptake capacity (mmol/g)	N_2 uptake capacity (mmol/g)	Selectivity
RUN380 (This work at 298K)	2.17	0.02	186
MgMOF-74	6.20	0.193	182.1
UTSA-16	2.37	0.043	314.7
NaX zeolite	2.72	0.106	145.9
Cu-SSZ13	1.78	0.150	67.4
H-SSZ13	1.74	0.138	71.3
JBW	1.42	0.015	524.4
mmenCuBTTri	2.22	0.038	329.0
ZnMOF-74	1.67	0.108	87.7
Bio-MOF-11	1.28	0.092	79.5
Cu-TDPAT	1.82	0.179	57.8
ZIF-78	0.76	0.1	41.4
MFI	0.26	0.134	11.2
MOF-177	0.16	0.245	3.6

Fig. S8 CO_2 heat of adsorption, Q_{st} of RUN380, estimated from low-pressure isotherms at 273 and 298 K by applying the Clausius-Clapeyron equation.

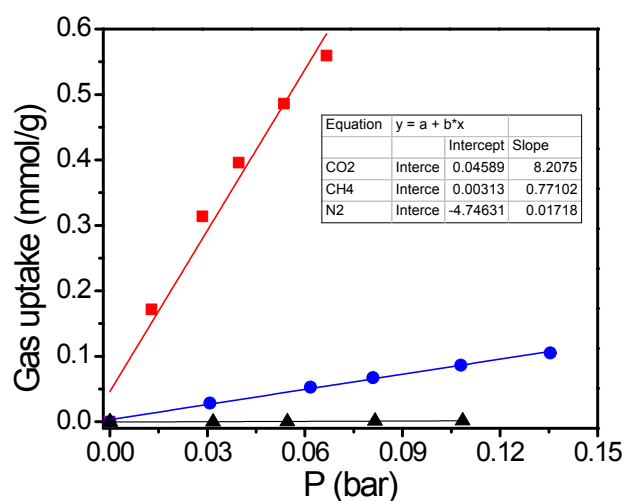| Equation	y = a + b*x		
		Intercept	Slope
CO2	Interce	0.04589	8.2075
CH4	Interce	0.00313	0.77102
N2	Interce	-4.74631	0.01718

Fig. S9 Initial slopes of single-gas adsorption isotherms. Adsorption selectivities of RUN380 for CO_2 (red square) relative to N_2 (black triangle) and relative to CH_4 (blue circle) at 298 K were calculated from these slopes.
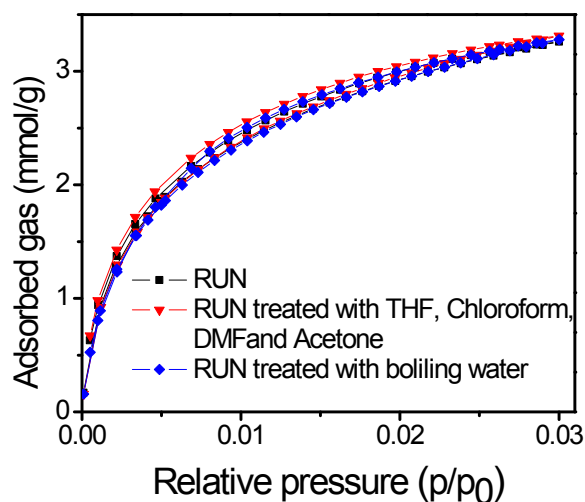
Fig. S10 CO_2 adsorption isotherms of an as-prepared RUN380 sample, that treated in boiling water, and that treated sequentially in boiling water, chloroform, DMF, and acetone. The stability of the RUN to water was investigated by having it refluxed in water for 3 days. After RUN were filtered and dried at 150 °C, its CO_2 adsorption isotherm was measured at 273 K and compared with that of the original RUN sample. The results showed that there was negligible change. We also checked it for solvent resistance. RUNs were soaked sequentially in THF, chloroform, DMF and acetone for 1 day, respectively, and then filtered and dried at 150 °C. There was negligible change in the measured CO_2 adsorption curves after solvent treatment.

References

(1)   S.-Y. Moon, E. Jeon, J.-S. Bae, M. Byeon, J.-W. Park, *Polym. Chem.* 2014, **5**, 1124-1131.

(2)   J. Mattia, P. Painter, *Macromolecules* 2007, **40**, 1546-1554.

(3)   H. G. Khorana, *Chem. Rev.* 1953, **53**, 145-166.

(4)   L. Stradella, M. Argentero, *Thermochimica Acta,* 1995, **268**, 1-7.

(5)   A. L. Myers, J. M. Prausnitz, *AIChE. J.* 1965, **11**, 121-127.

(6)   H. Furukawa and O. M. Yaghi, *J. Am. Chem. Soc.*, 2009, **131**, 8875-8883.

(7)   P. Pachfule, V. M. Dhavale, S. Kandambeth, S. Kurungot and R. Banerjee, *Chem. Eur. J*, 2013, **19**, 974-980.

(8)   T. Ben, C. Pei, D. Zhang, J. Xu, F. Deng, X. Jing and S. Qiu, *Energ. Environ. Sci*., 2011, **4**, 3991-3999.

(9)   R. Dawson, E. Stockel, J. R. Holst, D. J. Adams and A. I. Cooper, *Energ. Environ. Sci*., 2011, **4**, 4239-4245.

(10)   S. Xiang, Y. He, Z. Zhang, H. Wu, W. Zhou, R. Krishna and B. Chen, *Nat Commun*, 2012, **3**, 954.